12-1-2004

Manganese Oxide Thin Films Prepared by Nonaqueous Sol-Gel Processing: Preferential Formation of Birnessite

Stanton Ching
Connecticut College, sschi@conncoll.edu

Steven M. Hughes

Timothy P. Gray

Eric J. Welch

Recommended Citation

Stanton, C., Steven M., H., Timothy P., G., & Eric J., W. Manganese oxide thin films prepared by nonaqueous sol–gel processing: preferential formation of birnessite. *Microporous And Mesoporous Mater.*, **2004**, 7641-49. doi:10.1016/j.micromeso.2004.07.031

Manganese Oxide Thin Films Prepared by Nonaqueous Sol-Gel Processing: Preferential Formation of Birnessite

Stanton Ching,* Steven M. Hughes, Timothy P. Gray, Eric J. Welch

Department of Chemistry, Connecticut College, New London, CT 06320

ABSTRACT

High quality manganese oxide thin films with smooth surfaces and even thicknesses have been prepared with a nonaqueous sol-gel process involving reduction of tetraethylammonium permanganate in methanol. Spin-coated films have been cast onto soft glass, quartz, and Ni foil substrates, with two coats being applied for optimum crystallization. The addition of alkali metal cations as dopants results in exclusive formation of the layered birnessite phase. By contrast, analogous reactions in bulk sol-gel reactions yield birnessite, tunneled, and spinel phases depending on the dopant cation. XRD patterns confirm the formation of well-crystallized birnessite. SEM images of Li-, Na-, and K-birnessite reveal extremely smooth films having uniform thickness of less than 0.5 μm. Thin films of Rb- and Cs-birnessite have more fractured and uneven surfaces as a result of some precipitation during the sol-gel transformation. All films consist of densely packed particles of about 0.1 μm. When tetrabutylammonium permanganate is used instead of tetraethylammonium permanganate, the sol-gel reaction yields amorphous manganese oxide as the result of diluted Mn sites in the xerogel film. Bilayer films have been prepared by casting an overcoat of K-birnessite onto a Na-

birnessite film. However, Auger depth profiling indicates considerable mixing between the adjacent layers.

Keywords: birnessite, thin film, sol-gel, microporous manganese oxide

INTRODUCTION

Microporous manganese oxides continue to attract considerable scientific interest as inexpensive and non-toxic materials for potential use in heterogeneous catalysis, hazardous waste remediation, and rechargeable battery technology [1-4]. This large class of compounds with MnO_2 or near-MnO_2 stoichiometry displays a variety of structures based on edge-shared MnO_6 octahedra. Two examples of prevalent manganese oxides with microporous structures are shown in Figure 1. Birnessite is a layered material with alkali metal cations and water molecules typically residing in the interlayer region. Cryptomelane has a tunneled structure that contains interstitial potassium ions. Manganese oxides can be prepared by a wide array of synthetic methods, most of which require relatively mild reaction conditions [1-3].

Sol-gel processing has proven to be an effective route to microporous manganese oxides despite unconventional methodology. Traditional sol-gel condensation reactions have precluded manganese oxide syntheses due to a lack of suitable Mn(IV) molecular precursors. However, sol-gel processing can be carried out atypically through redox reactions between permanganate and organic reducing agents. Bach and co-workers were the first to establish a fully characterized sol-gel synthesis of a microporous manganese

oxide by preparing birnessite via reduction of fumaric acid in aqueous permanganate solution [5-7]. Ching and Suib later developed sol-gel routes to birnessite-type manganese oxide using aqueous sol-gel reactions between $KMnO_4$ or $NaMnO_4$ and saccharides (such as glucose and sucrose) as well as other polyalcohols (such as ethylene glycol and glycerol) [8, 9]. This work was built on much earlier observations of "manganese dioxide jellies" reported by Witzemann in 1915 [10]. With potassium-containing gels, there was an additional discovery that partial extraction of K^+ from the gel matrix led to formation of cryptomelane rather than birnessite [9, 11, 12]. More recently, Ching and Suib reported *nonaqueous* sol-gel routes to microporous manganese oxides using reactions of alkylammonium permanganates with methanol in the presence of alkali metal cations as dopants [13]. The nonaqueous gels served as precursors to manganese oxides with birnessite, cryptomelane, and spinel structures. (Manganese oxide spinels have a 3-D structure of edge-shared MnO_6 octahedra, which is derived from cubic close-packed oxygen with Mn in 1/2 of the octahedral holes and Li in 1/8 of the tetrahedral holes.)

Manganese oxide sol-gel chemistry has also found applications in thin films due to interest stemming from potential use related to battery cathodes, capacitors, and chemical sensors. However, compared to the conventional sol-gel condensation reactions that are routinely applied to silicon oxide and titanium oxide films [14, 15], the redox approach with manganese oxide gels faces challenges toward generating high quality thin films. In particular, reactions between permanganate and organic reducing agents leave considerable carbon-containing residue in the xerogel, which can easily cause the film to

fracture during drying and calcination. This situation is best illustrated in films prepared by aqueous sol-gel reactions using $KMnO_4$ and sucrose [16]. Such films are cast onto glass and Cu foil substrates by a variety of techniques including immersion, spray, spin, and spatula coating. After drying and calcination, the resulting films contain fractures and other coarse microscopic features on the order of tens of microns. Thin film products include birnessite, mixtures of birnessite with nonporous pyrolusite and ramsdellite phases, and amorphous manganese oxide.

In other sol-gel work, films with smoother and more uniform topographies have been obtained using dip-coating sol-gel methods that involve permanganate reduction with fumaric acid [17], hypochlorite oxidation of Mn(II) [17], permanganate oxidation of Mn(II) [18, 19], and alkylammonium permanganate reduction in aqueous 2-butanol [20]. Such procedures generate nonporous MnO_2 instead of microporous materials. Spinel-type $LiMn_2O_4$ films have also been prepared by reacting manganese acetylacetonate and lithium acetylacetonate in a 1-butanol/acetic acid solvent mixture, followed by spin coating [21, 22]. While described as sol-gel, this procedure also resembles the casting of a finely dispersed precipitate.

One of our goals in developing nonaqueous sol-gel routes to microporous manganese oxides is to explore the advantages of sol-gel processing with thin films. Aqueous sol-gel systems are not ideal for casting manganese oxide films because water has poor wetting characteristics on most surfaces. Nonaqueous sols should offer improvements in both film casting and quality. Herein, we report our findings on

nonaqueous sol-gel processing that yields manganese oxide thin films with the layered birnessite structure.

EXPERIMENTAL

Chemicals

Reagent grade chemicals were obtained commercially and used without further purification unless noted otherwise. Tetraethylammonium (TEA) bromide and tetrabutylammonium (TBA) bromide were purchased from Acros. Potassium permanganate was purchased from Fisher. Lithium acetate dihydrate, sodium acetate, potassium acetate, rubidium acetate, and cesium acetate were purchased from Aldrich. The highly hydroscopic rubidium and cesium acetates were handled in a Braun MB-50 glove box under a nitrogen atmosphere. Soft glass substrates were made from 1.2-mm thick glass microscope slides obtained from VWR Scientific. One-mm thick quartz slides and 0.127-mm thick Ni foil were obtained from Chem Glass and Strem, respectively. HPLC grade methanol solvent was purchased from Fisher. Distilled deionized water was obtained from a Barnsted Nanopure II water purification system and used throughout. $TEAMnO_4$ and $TBAMnO_4$ were prepared by metathesis reactions between $KMnO_4$ and alkylammonium bromide in water [13]. Solutions of $KMnO_4$ were filtered through a medium porosity glass frit prior to reaction. The alkylammonium permanganates were dried under vacuum at room temperature and refrigerated in storage to delay thermal decomposition. $TEAMnO_4$ and $TBAMnO_4$ are not considered explosion hazards among the alkylammonium permanganates, but as a general precaution they were

never handled above ambient temperature. SAFETY PRECAUTION: We considered using tetramethylammonium permanganate ($TMAMnO_4$) as an additional permanganate reactant. However, on one occasion this compound detonated upon being synthesized at room temperature. Therefore, we avoided its use out of safety concerns, although $TMAMnO_4$ is not cited in the literature as an explosion hazard.

Manganese Oxide Thin Films

Manganese oxide sols were spin coated onto approximately 2.5-cm square substrates using a Chemat KW-4B spin coater. Soft glass and quartz glass slides were pre-treated by sequential cleaning with acetone, concentrated sulfuric acid, and acetone. Ni foil substrates were cleaned with acetone only. Manganese oxide sol-gels were prepared by dissolving alkali metal acetate salts (0.28 mmol for Li^+, Na^+, Rb^+, Cs^+; 0.14 mmol for K^+) in 3 mL of methanol, then adding 0.14 g (0.56 mmol) of solid $TEAMnO_4$. The purple slurry eventually dissolved into a red-brown sol with regular swirling. Spin coating was carried out when the sol turned brown (20-50 min, depending on the alkali cation). A total of 7-8 drops of sol were applied by pipette as the substrate was spun initially at 750 rpm for 10 s. The substrate was then spun at 1500 rpm for an additional 10 s. The film was dried for at least 1 h at 110 ºC before a second sol-gel coat was applied. Films were finally calcined at 450 ºC for 1 h. Once cooled, the films were rinsed with water.

Characterization

Powder X-ray diffraction (XRD) measurements were performed with a Rigaku MiniFlex powder X-ray diffractometer using Cu Kα radiation. Samples were scanned at

5° 2θ/min. Beam voltage and beam current were 30 kV and 15 mA, respectively. Scanning electron microscopy images were obtained using a LEO model 435VP SEM. Samples were sputter coated with Pd/Au, except when also subjected to EDAX analysis. Samples for edge-on images were prepared by fracturing the glass substrate after scoring the uncoated side. Elemental analyses for Li, Na, and K were performed by atomic absorption spectroscopy using a Perkin Elmer model 2380 AA spectrometer. Thin film samples were digested using a minimum amount of 4:1 v/v 30% H_2O_2:0.1 M HCl. Soft glass was used as the substrate for Li measurements, while quartz substrates were used for Na and K. Typically, 5-6 thin films were combined to provide sufficient sample for one analysis. Elemental analyses for Rb and Cs were obtained by energy dispersive X-ray spectroscopy using an Oxford Link EDAX analyzer. Auger electron spectroscopy with Ar-sputtered depth profiling was performed using a Perkin-Elmer PHI 610 scanning Auger microprobe. Thermogravimetric analyses were carried out using a TA Instruments model Q50 TGA. Films were cast onto thin glass cover slips, which were heated together at a rate of 20 °C/min.

RESULTS

Preparation of Birnessite Thin Films

Nonaqueous sols are generated by reduction of $TEAMnO_4$ in methanol. The sols are then cast as thin films by spin coating. Optimum homogeneity and crystallinity are achieved by applying two spin coats prior to calcination. The dried xerogel films are amorphous, but become crystalline upon calcination at 450 °C. This procedure has been

applied to soft glass, quartz glass, and Ni foil substrates. Sample films are shown in Figure 2. Birnessite-type manganese oxides are obtained on soft glass using sol-gel films with alkali metal cations added as dopants (Li^+, Na^+, K^+, Rb^+, or Cs^+). In the absence of alkali dopants, the process yields thin films of nonporous Mn_2O_3. Reactions are carried out with alkali metal:Mn ratios of 0.5:1 except for K^+, which gives the best results with a 0.25:1 K:Mn ratio. Birnessite forms similarly on quartz and Ni foil, except for Li-doped sol-gel films, which are amorphous.

Crystallinity

Powder XRD patterns of birnessite thin films on soft glass substrates are shown in Figure 3. The interlayer distance is similar for Li-, Na-, and K-birnessite films: 6.90 Å, 6.99 Å, and 6.96 Å, respectively. The spacing increases slightly for Rb and Cs-birnessite: 7.13 Å and 7.28 Å, respectively. In the preparation of Li and Na-doped films, the product initially characterized by XRD is a dehydrated form of birnessite, which has an interlayer spacing of 5.5 Å. Brief exposure to water or prolonged exposure to ambient humidity results in conversion to the hydrated 7 Å birnessite phase, Figure 4. The process is reversible as the 5.5 Å phase easily regenerates from 7 Å birnessite by mild heating at 110 °C for about one hour. This also occurs for films on quartz and Ni foil.

Smoothness and Thickness

SEM images of thin films on glass are displayed in Figures 5 and 6. Na- and K-birnessite films appear smooth and evenly coated, even under high magnification, Figures 5b and 5c. Li-birnessite films are similarly well formed, except for the occurrence of 0.5-μm boils where the film lifts away from the substrate, Figure 5a. By contrast, Rb- and

Cs-birnessite films display considerable fracturing and a significantly more coarse topography, Figures 5d and 5e. The smoothness of the thin films correlates with the homogeneity of their corresponding sols. The sols with Li^+, Na^+, and K^+ dopants are homogeneous, whereas those having Rb^+ and Cs^+ dopants contain finely divided precipitate. The fractured areas of Rb- and Cs-birnessite films are dispersed similarly to the microscopic precipitate particles observed on these films prior to calcination.

Edge-on views reveal sub-micron thickness for all of the birnessite thin films, Figure 6. The images of Li-, Na-, and K-birnessite films show uniform coatings with thicknesses of less than 0.5 μm. The Li-birnessite image also shows how small sections of film lift away from the substrate to create the circular boils observed in Figure 5a. Rb- and Cs-birnessite films are thicker, ranging from 0.5-1.0 μm. Their fractured surfaces are again evident as they were in Figures 5d and 5e. All the birnessite films consist of densely packed grains that are roughly 0.1 μm in diameter or less.

SEM images of birnessite on Ni foil reveal similar characteristics to those on glass. An example with Na-birnessite is shown in Figure 7. The surface of the film is smooth and well formed, although the contour of the Ni foil is not as even as it is for glass. Since Ni does not cleave as easily as glass, edge views were obtained by cutting the foil with metal snips, which causes nearby areas of the film to fracture and lift from the substrate. The film thickness on Ni foil is less than 0.5 μm.

Composition

Alkali-metal-to-manganese ratios for the thin films have been determined by AA and EDAX analyses. AA was used to analyze Li-birnessite on soft glass and for Na- and

K-birnessite on quartz. Analyte solutions were prepared by combining samples from several films. The Rb- and Cs-birnessite films were analyzed using EDAX measurements. Alkali:Mn ratios for the birnessite thin films were found to be Li(0.10), Na(0.30), K(0.24), Rb(0.24), and Cs(0.26).

Thermal Analysis

Calcination of thin film xerogels was examined by TGA. Films were cast onto glass cover slips, enabling analyses of the films while still attached to the substrate. TGA studies of thin films during calcination reveal two scenarios, Figure 8. Li-, Na-, and K-doped films undergo a single weight loss event in the 150-250 ºC range. A typical TGA trace is shown for the Li-doped xerogel film, Figure 8a. Rb- and Cs-doped films experience two weight loss events, one from 150-230 ºC and another from 270-370 ºC. The TGA trace for a Cs-doped film is shown in Figure 8b.

The thermal stability of manganese oxide thin films was investigated for Na-, K-, Rb-, and Cs-birnessite on quartz. Films were heated at 600, 700, and 800 ºC for 1 hour each. Based on the resulting XRD patterns, Na-birnessite was the least stable film, completely decomposing to Mn_3O_4 at 600 ºC whereas little or no change occurred for the other films. At 700 ºC, the Cs-birnessite film mostly converted to Mn_3O_4, while K- and Rb-birnessite showed evidence of Mn_3O_4 formation. At 800 ºC, all films had fully converted to Mn_3O_4. No intermediate phases were observed.

Bilayer Films

A Na-doped sol-gel film was applied to Ni foil to generate a Na-birnessite undercoat. The same procedure was then performed with a K-doped film to create a K-

birnessite overlayer. The XRD pattern of this proposed bilayer film is shown in Figure 9. Since Na-birnessite initially forms as the dehydrated 5.5 Å phase, its XRD pattern is easily distinguished from that of 7 Å K-birnessite. Exposure to ambient air slowly converts the 5.5 Å layered phase into 7 Å Na-birnessite over the course of 30-60 minutes. Brief soaking in water promotes rapid interlayer hydration.

SEM images reveal smooth and evenly coated films that are about 1.5-times thicker than films with just one type of birnessite coating. However, there is no evidence of distinct Na- and K-birnessite layers. Depth profiling by Auger electron spectroscopy provides some indication of bilayer formation, since initial surface analyses show the presence of K but not Na, Figure 10. However, deeper profiling provides clear evidence of mixing between the Na- and K-containing layers as the Na:Mn ratio increases while the K:Mn ratio decreases. Eventually, both ratios diminish until the underlying Ni substrate is reached.

DISCUSSION

Thin Film Preparation

Spin coating with nonaqueous sol-gel mixtures provides an excellent route to manganese oxide thin films of high quality in terms of crystallinity, smoothness, and uniform thickness. There is also a unique selectivity for birnessite, even though a variety of microporous phases are obtained when identical reactions are carried out in bulk. For example, sol-gel reactions with Li^+ dopant ordinarily generate spinel manganese oxide in both aqueous [3] or methanol [31] solvent. Similarly, cryptomelane has been obtained in

bulk from K-doped gels having a 0.25:1 K:Mn ratio [13], while this same ratio favors K-birnessite when the gel is cast as a thin film. K-birnessite is only favored in bulk sol-gel synthesis when the K:Mn ratio is raised to 0.5:1 [13]. These results implicate some sort of mechanism in which the smooth substrate surface promotes the formation of lamellar manganese oxide structure upon crystallization. There is remote similarity to epitaxial film growth on single crystal substrates, but the manganese oxide system clearly has a different influence since the glass substrates are not crystalline. The same spin coated films on identically treated ground glass substrates are amorphous. Unfortunately, the reason for this preferential formation of layered manganese oxide structure has not been elucidated. Lamellar manganese oxide is favored in films derived from colloidal suspensions, but in these cases the crystallinity is either established immediately during colloid formation [23, 24] or pre-exists from an exfoliated precursor [25-29].

Attempts to prepare crystalline thin films by substituting $TBAMnO_4$ for $TEAMnO_4$ in the sol-gel process have been unsuccessful. Although the $TBAMnO_4$-derived films are generally indistinguishable from their $TEAMnO_4$ counterparts, XRD analyses show amorphous manganese oxide product. It is believed that a critical Mn concentration is needed in the xerogel film to promote crystallization during calcination. The dilution of Mn sites, caused by the increased organic content in TBA^+-containing films, is evidently sufficient to inhibit crystallization. By contrast, bulk sol-gel syntheses yield identical results with either $TBAMnO_4$ or $TEAMnO_4$. Thus, it appears that Mn concentration is critical only if Mn sites are very limited, such as in thin films.

The formation of Li-birnessite on soft glass, but not on quartz or Ni foil, is also an unresolved observation. One speculation is that Li-doped gels extract some of the Na^+ and K^+ inherent to the soft glass, prompting formation of small quantities of Na- and K-birnessite at the gel/surface interface. This in turn nucleates growth of Li-birnessite. Such a pathway is not available on quartz and Ni foil, which lack alkali metal cations. Attempts to generate Li-birnessite on quartz and Ni foil by intentionally adding Na^+ or K^+ to Li-containing gels have been unsuccessful.

Characterization

The XRD patterns of birnessite thin films in Figure 3 show the excellent crystallinity of these materials. The approximate 7 Å interlayer distances are indicative of birnessite-type manganese oxides and the increased spacing associated with larger alkali metal cations is consistent with other studies involving synthetic birnessites [30]. Elemental analyses reveal alkali metal:Mn ratios that are in general agreement with the 0.25-0.35 range typically observed for birnessite materials. The notable exception is the low 0.10 Li:Mn ratio.

The application of two spin coats plays a key role in achieving highly crystalline thin films. XRD peak intensities are 2-5 times greater compared to films prepared from a single spin coat. Additional coatings do not yield further improvement in film quality. While the increase in XRD intensity can be partially attributed to increased film thickness, comparisons of XRD and SEM results from singly and doubly coated films clearly suggest there are other contributions. Denser particle packing in the film can enhance XRD intensities, but there is no indication of this from SEM observations. Thus,

the second spin coating is believed to improve the crystalline quality of the birnessite particles in addition to increasing the thickness of the film.

SEM analyses reveal exceptionally smooth surfaces for Li-, Na-, and K-birnessite films, Figure 5. Edge-on views of the 0.3-0.5 μm thick films show that they consist of densely packed grains on the order of 0.1 μm, Figure 6. The particle morphology is identical to that of nonaqueous sol-gel birnessite from bulk syntheses and is similar to amorphous MnO_2 observed in films prepared by reduction of tetrapropylammonium permanganate with aqueous 2-butanol [20] and by $KMnO_4$ reduction with Mn(II) [18]. By comparison, Rb- and Cs- birnessite films are considerably fractured. This coarse topography is attributed to precipitation that accompanies the sol-gel transition. Indeed, SEM images of Rb- and Cs-birnessite films show that precipitated particles observed on the surface prior to calcination have similar size and dispersion to the factured areas after calcination.

TGA measurements of birnessite films supported on glass cover slips show a common weight loss event at 150-250 ºC, which corresponds to calcination of residual organics. Tetraethylammonium acetate, which represents much of the organic content in the film, calcines over the same temperature range. The higher temperature weight loss observed only in TGA measurements of Rb- and Cs-doped films has been assigned to calcination of the microscopic precipitate residing on these films. As further evidence, the precipitated particles are observed in SEM images of uncalcined Rb- and Cs-doped films and persist after calcination at 250 ºC. However, the surface particles are no longer evident after calcination at 450 ºC, which coincides with the appearance of fracturing.

All the films require calcination at 450 ºC to achieve optimum birnessite crystallinity. Lower temperatures result in weakly crystalline or amorphous films.

The thermal stability of the thin film birnessites differs somewhat from the thermal behavior of analogous compounds obtained in powdered bulk forms. The ultimate decomposition to Mn_3O_4 at 800 ºC is typical of birnessite and most other microporous manganese oxides. However, the absence of observed intermediates in all cases is unusual. In particular, Li-birnessite has shown a propensity for the spinel form at temperatures ranging from 110 ºC to 600 ºC [5, 31, 32]. K-birnessite is known to transform into cryptomelane at temperatures in the range of 500-600 ºC [12], although this conversion was not observed in nonaqueous bulk sol-gel syntheses [13].

Comparison with Films for Aqueous Sol-Gel Reactions

The quality of birnessite thin films from nonaqueous sol-gel processing easily surpasses that of films prepared by analogous procedures with aqueous gels. This success is attributed to superior surface wetting afforded by nonaqueous sols, which promotes a more uniform coating. Aqueous sol-gel mixtures yield amorphous manganese oxide films when spin coated onto glass and Cu foil [16]. Crystallinity is achieved only for thicker films applied by immersion, spray, and spatula coating methods. However, these films have coarse and fractured topographies, even more so than the Rb- and Cs-birnessite thin films prepared by nonaqueous sol-gel processing.

Another critical factor for improved film quality is the gelation time. Aqueous sol-gel reactions of permanganate with saccharides and other polyalcohols reach the gel stage within two minutes of reactant mixing [9, 16]. The useable time window for

casting films before the onset of gelation is only about 30 seconds. This presents a significant challenge to being able to cast the film after all the permanganate has reacted but also before the sol becomes too viscous. By contrast, the nonaqueous process requires 30-60 minutes for gelation, depending on the alkali dopant. The usable time window in the sol stage is a relatively generous 10-15 minutes, allowing for greater care in casting the films.

Birnessite Bilayers

The exceptional smoothness of Na- and K-birnessite thin films, along with their apparent strong adherence to substrates, spurred an investigation of birnessite bilayers. Ni foil was chosen for these experiments because film adherence seems particularly tenacious on this substrate. Bilayers consisting of a Na-birnessite undercoat and K-birnessite overlayer give no indication of discrete layers by SEM analysis. However, the birnessites are distinguishable by XRD since only Na-birnessite forms the dehydrated 5.5 Å phase. The eventual conversion of Na-birnessite to its hydrated 7 Å phase demonstrates the permeability of the K-birnessite overlayer to water. Auger elemental depth profiling reveals segregation of the Na- and K-containing layers at the surface of the film, where potassium is detected without the presence of sodium. However, substantial mixing occurs below, with significant concentrations of both sodium and potassium being detected at the same time. Thus, the separate application of Na- and K-containing sol-gel layers does not prevent the layers from intermingling.

CONCLUSIONS

Nonaqueous sol-gel processing is an effective method of producing high quality thin films of manganese oxide with selectively for the layered birnessite structure. The reduction of $TEAMnO_4$ in methanol in the presence of dopant alkali metal cations offers a favorable route to sols that are readily cast onto soft glass, quartz glass, and Ni foil substrates. The same reaction cannot be carried out using $TBAMnO_4$, presumably due to a sub-critical density of Mn sites required for crystallization. The exclusive formation of birnessite is in contrast to analogous sol-gel syntheses in bulk, which yield a variety of microporous products with layered, tunneled, and spinel structures. Li-, Na-, and K-birnessite films are particularly smooth and well formed, with thicknesses of less than 0.5 μm. Rb- and Cs-birnessite films have relatively coarse topographies due to granular precipitation occurring in the sol. Bilayer films with Na- and K-birnessite can be prepared, but there is considerable mixing of the layers.

ACKNOWLEDGMENTS

We gratefully acknowledge generous support for this research from the National Science Foundation (Grant # 0209688), the Research Corporation, and the American Chemical Society–Petroleum Research Fund. The Keck Foundation is also acknowledged for providing summer stipends for SMH and EJW. We also thank Dr. Bill Willis and Professor Steven L. Suib at the University of Connecticut for performing the Auger analysis.

REFERENCES

[1] Q. Feng, H. Kanoh, K. Ooi, J. Mater. Chem. 9 (1999) 319.

[2] S.L. Brock, N. Duan, Z.R. Tian, O. Giraldo, H. Zhou, S.L. Suib, Chem. Mater. 10 (1998) 2619.

[3] A. Manthiram, J. Kim, Chem. Mater. 10 (1998) 2895.

[4] M.M. Thackeray, J. Electrochem. Soc. 142 (1995) 2558.

[5] S. Bach, M. Henry, N. Baffier, J. Livage, J. Solid State Chem. 88 (1990) 325.

[6] P. Le Goff, N. Baffier, S. Bach, J.P. Pereira-Ramos, R. Messina, Solid State Ionics 61 (1993) 309.

[7] P. Le Goff, N. Baffier, S. Bach, J.P. Pereira-Ramos, Mater. Res. Bull. 31 (1996) 63.

[8] S. Ching, J.A. Landrigan, M.L. Jorgensen, N. Duan, S.L. Suib, C.L. O'Young, Chem. Mater. 7 (1995) 1604.

[9] S. Ching, D.J. Petrovay, M.L. Jorgensen, S.L. Suib, Inorg. Chem. 36 (1997) 883.

[10] E.J. Witzemann, J. Am. Chem. Soc. 37 (1915) 1079.

[11] N. Duan, S.L. Suib, C.L. O'Young, J. Chem. Soc. Chem. Commun. (1995) 1367.

[12] S. Ching, J.L. Roark, N. Duan, S.L. Suib, Chem. Mater. 9 (1997) 750.

[13] S. Ching, E.J. Welch, S.M. Hughes, A.B.F. Bahadoor, S.L. Suib, Chem. Mater. 14 (2002) 1292.

[14] L.F. Francis, in N.B. Dahotre, T.S. Sudarshan (Eds.), Intermetallic and Ceramic Coatings, Materials Engineering Series, Vol. 13, Marcel Dekker, New York, 1999, pp. 31-82.

[15] S. Sakka, T. Yoko, Struct. Bonding 77 (1992) 89.

[16] S.R. Segal, S.H. Park, S.L. Suib, Chem. Mater. 9 (1997) 98.

[17] H.P. Stadniychuk, M.A. Anderson, T.W. Chapman, J. Electrochem. Soc. 143 (1996) 1629.

[18] S.C. Pang, M.A. Anderson, J. Mater. Res. 15 (2000) 2096.

[19] S.C. Pang, M.A. Anderson, T.W. Chapman, J. Electrochem. Soc. 147 (2000) 444.

[20] S.F. Chin, S.C. Pang, M.A. Anderson, J. Electrochem. Soc. 149 (2002) A379.

[21] Y.J. Park, J.G. Kim, M.K. Kim, H.T. Chung, W.S. Um, M.H. Kim, H.G. Kim, J. Power Sources 76 (1998) 41.

[22] Y.J. Park, J.G. Kim, M.K. Kim, H.T. Chung, H.G. Kim, Solid State Ionics 130 (2000) 203.

[23] S.L. Brock, M. Sanabria, S.L. Suib, V. Urban, P. Thiyagarajan, D. Potter, J. Phys. Chem. B 103 (1999) 7416.

[24] S.L. Brock, M. Sanabria, J. Nair, S.L. Suib; T. Ressler, J. Phys. Chem. B 105 (2001) 5404.

[25] Z.H. Liu, X. Yang, Y. Makita, K. Ooi, Chem. Lett. (2002) 680.

[26] Z. H. Liu, X. Yang, Y. Makita, K. Ooi, Chem. Mater. 14 (2002) 4800.

[27] Y. Omomo, T. Sasaki, L. Wang, M. Watanabe, J. Am. Chem. Soc. 125 (2003) 3568.

[28] L. Wang, Y. Omomo, N. Sakai, K. Fukuda, L. Nakai, E. Yasuo, K. Takada, M. Watanabe, T. Sasaki, Chem. Mater. 15 (2003) 2873.

[29] L. Want, K. Takada, A. Kajiyama, M. Onoda, Y. Michiue, L. Zhang, M. Watanabe, T. Sasaki, Chem. Mater. 15 (2003) 4508.

[30] H. Kanoh, W. Tang, Y. Makita, K. Ooi, Langmuir 13 (1997) 6845.

[31] R. Chen, M. S. Whittingham J. Electrochem. Soc. 144 (1997) L64.

[32] J. Morales, L. Sanchez, S. Bach, J. P. Pereira-Ramos Mater. Lett. 56 (2002) 653.

FIGURE CAPTIONS

Figure 1. Structures of microporous manganese oxides: layered birnessite and tunneled cryptomelane. The interlayer spacing for birnessite is 7 Å and the tunnel dimension of cryptomelane is 4.6 Å x 4.6 Å.

Figure 2. Na-birnessite thin films on glass (left) and Ni foil (right). The substrates are roughly 2.5 cm x 2.5 cm.

Figure 3. XRD patterns of Li-, Na-, K-, Rb-, and Cs-birnessite thin films on glass.

Figure 4. XRD patterns and structures of (a) dehydrated 5.5 Å Na-birnessite; (b) hydrated 7 Å Na-birnessite.

Figure 5. Top view SEM images of birnessite thin films on glass: (a) Li-birn; (b) Na-birn; (c) K-birn; (d) Rb-birn; (e) Cs-birn.

Figure 6. Edge view SEM images of birnessite thin films on glass: (a) Li-birn; (b) Na-birn; (c) K-birn; (d) Rb-birn; (e) Cs-birn.

Figure 7. SEM images of Na-birnessite thin film on Ni foil: (a) top view; (b) edge view.

Figure 8. TGA analyses of sol-gel thin films on glass: (a) Li-doped; (b) Cs-doped. Note: the films are supported on glass cover slips that account for nearly all the sample mass.

Figure 9. XRD pattern of Na-birnessite/K-birnessite bilayer film on Ni foil. The peaks are marked to show 7 Å K-birnessite (*) and 5.5 Å Na-birnessite (#).

Figure 10. Auger electron spectroscopy depth profile for Na-birnessite/K-birnessite bilayer film on Ni foil. The vertical axis tracks the alkali-metal-to-Mn elemental ratio. Squares represent K:Mn ratios and triangles represent Na:Mn ratios.

Figure 1

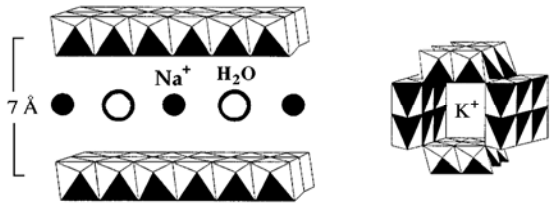

Figure 2

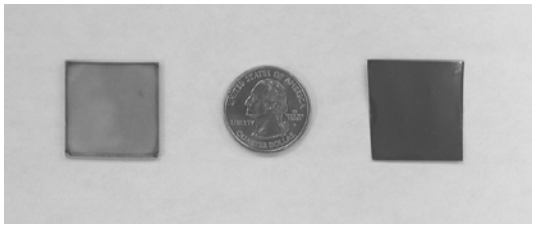

Figure 3

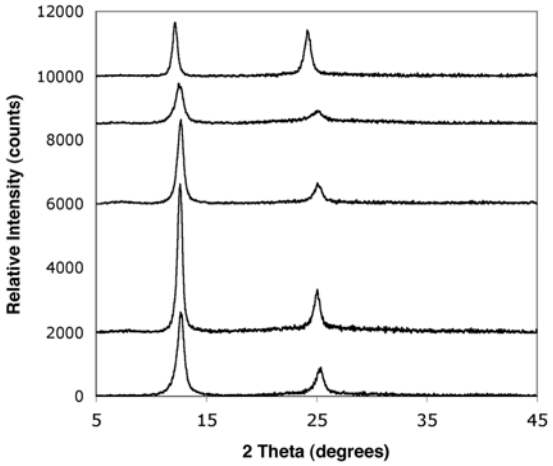

Figure 4

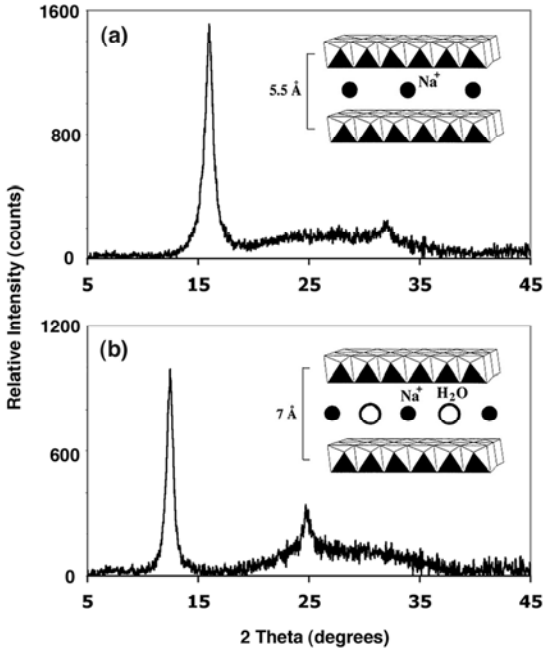
(a)
1600
800
0
5.5 Å
Na+
(b)
1200
600
0
7 Å
Na+
H2O
5
15
25
35
45
Relative Intensity (counts)
2 Theta (degrees)

Figure 5

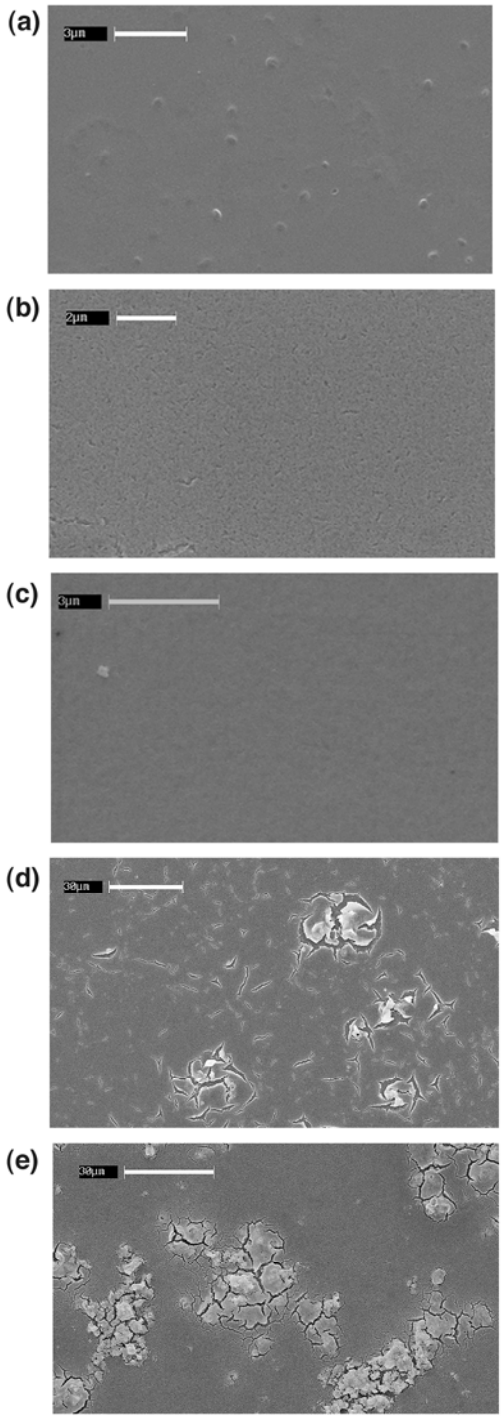

Figure 6

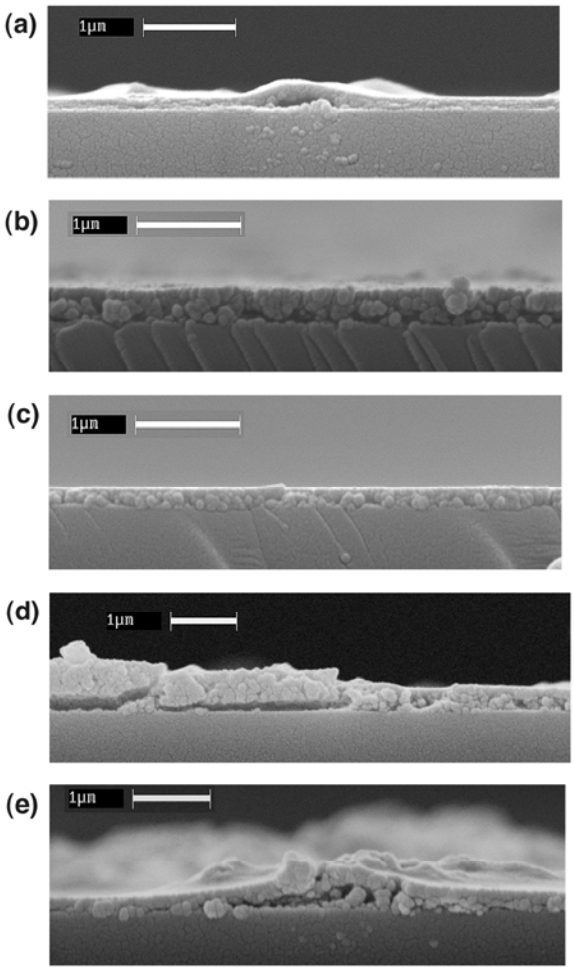

Figure 7

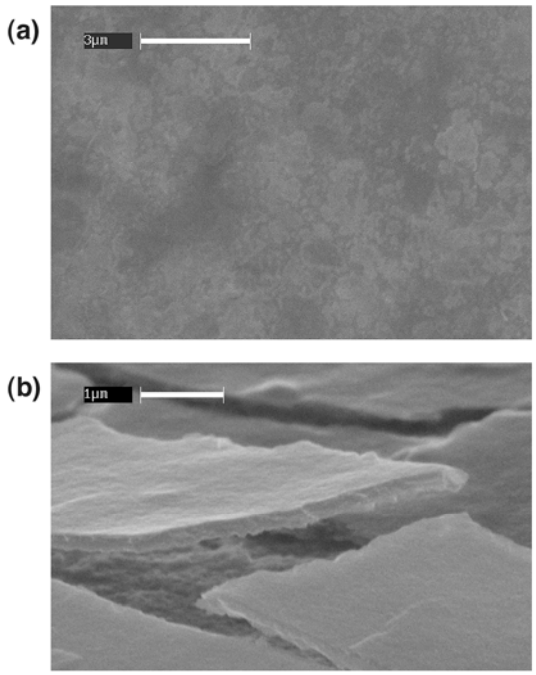

Figure 8.

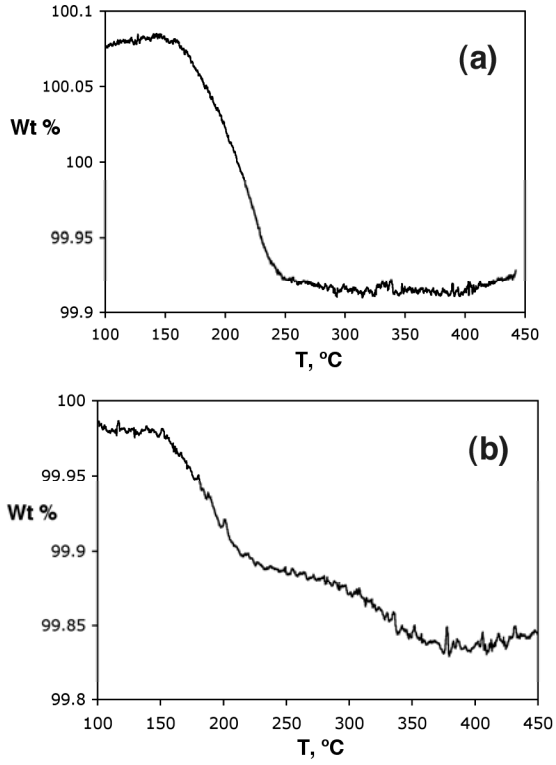

Figure 9

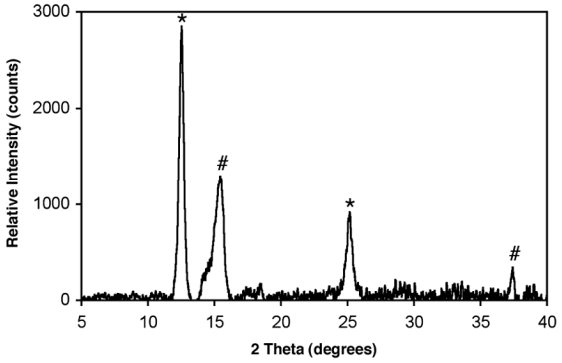

Figure 10